Crystal fields and dopant-ligand separations in cubic centres of rare-earth ions in fluorites

1990 J. Phys.: Condens. Matter 2 5563

(http://iopscience.iop.org/0953-8984/2/25/008)

J. Phys.: Condens. Matter 2 (1990) 5563–5574. Printed in the UK

Crystal fields and dopant–ligand separations in cubic centres of rare-earth ions in fluorites

K Leśniak
Institute of Physics, Polish Academy of Sciences, Al. Lotników 32/46, 02-668 Warszawa, Poland

Received 12 December 1989, in final form 23 February 1990

Abstract. Phenomenological crystal-field parameters were calculated from spectroscopic data for Eu^{3+}, Dy^{3+} and Er^{3+} in cubic sites in a number of fluorite-structure hosts. These values, and similar data from other calculations, were used to obtain, with the help of a semi-empirical modelling procedure, the dopant–ligand distances in the corresponding centres. It is confirmed that significant local lattice collapse does take place in these centres. The final dopant–ligand distances calculated in this investigation compare favourably with relevant information collected by other methods.

1. Introduction

Past investigations [1] of the numerous and diverse centres appearing when trivalent rare-earth ions (RE^{3+}) are substituted for the divalent lattice cations of fluorite-structure crystals showed that this type of substitution is accompanied by significant local host-lattice distortions. In the present work, an attempt is made to reconstruct these distortions in the case of the cubic centres in these host:lattice systems. To achieve this, a modelling procedure was developed that starts from the phenomenological crystal-field parameter values for the cubic centre of interest, and translates these into information about local host-lattice distortions.

The cubic centres of RE^{3+} dopants in fluorite-structure hosts are distinguished from the other centres in these host-lattice systems by the fact that their local structures are particularly simple. Thus, the local environment of the dopant in a centre of this type consists of just eight F^- ligands in a cubic arrangement around the RE^{3+} ion. Such systems have been studied for a long time by both optical and electron spin resonance (ESR) techniques [2–5], with recent site-selective excitation studies confirming the long-held view that, in a number of fluorite-structure hosts, the cubic sites are among the major ones [6–9].

Accumulation of spectroscopic data on these systems has, nevertheless, been slow, since the relevant optical signals are weak as a result of the presence of inversion symmetry in the O_h local symmetry group. In fact, even now, no satisfactory optical data appear to be available for a number of these dopant:lattice systems. Furthermore, even in cases when such data are available, only two independent non-zero phenomenological crystal-field parameter values are obtained when the energy level scheme of the relevant spectrum is parametrised. This limited number of phenomenological parameter values

0953-8984/90/255563 + 12 $03.50

places a severe constraint on the amount of information that a modelling procedure may be expected to yield. The above considerations make the task of microscopic local structure simulation for cubic centres as challenging as for the structurally more complicated tetragonal centres in these host:lattice systems, for which an analogous procedure was developed in the past [10, 11].

The basis of our work was thus the phenomenological crystal-field parameters, calculated using optical data for a number of cubic centres in various RE^{3+}:fluorite systems. The results of such calculations, performed in the course of this investigation, are reported in section 2. The procedure employed in translating these parameter values into local lattice distortions is presented in section 3. This presentation is followed by a discussion of the results obtained, and their comparison with relevant information obtained in other studies of these centres (section 4).

2. Phenomenological analysis of selected spectra

The aims outlined in section 1 place some constraints on the phenomenological crystal-field parameter values to be used in our work. Thus, we focus our attention on cases where appropriate data for a given dopant are available for several fluorite hosts. In such cases, changes in dopant–ligand separation across the isostructural fluorite series may be investigated. These changes are often easier to establish reliably than the relevant absolute distances and, in particular, our results may thus be compared with suitable values obtained from magnetic resonance data. Clearly, we also require that the computational procedures used to parametrise the spectra be the same for all the cubic centres associated with a given RE^{3+} dopant.

A search through the literature showed that suitable data appear to be available for Tb^{3+} [12] and Gd^{3+} [13]. For three other dopants (Er^{3+}, Dy^{3+} and Eu^{3+}), the phenomenological values of crystal-field parameters used in further analysis were calculated in the course of this investigation.

The crystal-field parameters employed are the B_q^k parameters defined by Wybourne [14]. For cubic symmetry systems, only two of these (B_0^4 and B_0^6) are independent and non-vanishing. In the cases when determination of phenomenological values of B_q^k was performed in this study, effects of intermediate coupling were accounted for by using the reduced matrix elements of Carnall *et al* [15]. For Eu^{3+}, the fitting was performed using a perturbation matrix containing all the states of the ^7F term, with the J-mixing effect accounted for. For Dy^{3+}, the crystal-field matrix consisted of states of the two lowest J-manifolds ($^6H_{15/2}$ and $^6H_{13/2}$). In this case, J-mixing was neglected. The reasons for such truncation of the diagonalisation basis will be given in section 2.2. For Er^{3+}, the B_q^k parameter values were determined using a crystal-field matrix consisting of states of the lowest ($^4I_{15/2}$) manifold. In all these cases, the fitting was performed by minimising the root-mean-square (RMS) deviation between the calculated and observed level energies. The quantity used to assess the quality of the final results is the adjusted RMS deviation σ, defined as

$$\sigma = \left(\sum_i (E_{i,c} - E_{i,e})^2/(n-p) \right)^{1/2}$$

where $E_{i,c}$, $E_{i,e}$, n and p are, respectively, the calculated and measured energies of level i, the number of levels observed and the number of independent fitting parameters.

2.1. Determination of phenomenological values of B_q^k for Eu^{3+}

The principal difficulty in determination of phenomenological values of B_q^k for Eu^{3+} lies in collecting sufficient experimental data on the energy levels of this dopant in cubic symmetry centres. The difficulties noted in section 1, present for all cubic centres, are in this case compounded by the low multiplicities of the low-lying J-manifolds of Eu^{3+}. The end result is that suitable information collected in site-selective studies of this dopant in CaF_2 [7] and BaF_2 [16] is insufficient to determine phenomenological values of B_q^k for Eu^{3+} in cubic sites in these hosts.

Fortunately, the situation is somewhat better for cubic centres in other fluorite-structure crystals. For CdF_2, site-selective studies [8, 17] yielded the energies of pairs of levels from the $^7F_2$ and $^7F_3$ manifolds of Eu^{3+} in cubic sites, and these data just suffice to calculate the phenomenological values of B_0^4 and B_0^6. Analogous data were also collected for Eu^{3+}-doped SrF_2 [18] and PbF_2 [9].

In view of the limited energy level data available to determine phenomenological B_q^k, as well as the non-linearity of the fitting procedure, choice of the values of B_q^k from which to start the minimisation procedure becomes of particular importance in this case. We tackled this problem by calculating σ for a number of different initial values of B_0^4 and B_0^6, and starting the minimisation from the two sets of B_q^k that corresponded to the two lowest values of σ. Thus, for PbF_2 the initial values of B_0^4 extended from -1700 to $-2100\ cm^{-1}$, and those of B_0^6 from $+300$ to $+900\ cm^{-1}$ (in steps of $100\ cm^{-1}$), with each pair of B_0^4 and B_0^6 in this range examined. For SrF_2, the corresponding initial values of B_0^4 ranged from -1800 to $-2200\ cm^{-1}$, and those of B_0^6 from $+500$ to $+900\ cm^{-1}$ (in steps of $100\ cm^{-1}$). For CdF_2, a similar procedure was at first followed, with initial B_0^4 and B_0^6 values being chosen from a grid of (B_0^4, B_0^6) points, with $100\ cm^{-1}$ separation. The starting B_q^k values thus chosen, however, turned out to lead to a final value of σ that was significantly higher than those for PbF_2 and SrF_2. The situation only changed when separation of points on the initial (B_0^4, B_0^6) grid was reduced to $50\ cm^{-1}$, B_0^4 ranging from -1800 to $-2400\ cm^{-1}$, and B_0^6 from $+500$ to $+900\ cm^{-1}$.

The starting values of B_q^k thus determined were (in cm^{-1}): $B_0^4 = -2000$, $B_0^6 = +500$, and $B_0^4 = -2000$, $B_0^6 = +400$ (PbF_2); $B_0^4 = -2000$, $B_0^6 = +600$, and $B_0^4 = -2000$, $B_0^6 = +700$ (SrF_2); $B_0^4 = -2300$, $B_0^6 = +700$, and $B_0^4 = -2250$, $B_0^6 = +800$ (CdF_2). After the minimisation procedure, the final values of B_q^k (chosen to be those corresponding to lowest σ) were found to be (in cm^{-1}): $B_0^4 = -2256$ and $B_0^6 = +798.8$ (CdF_2); $B_0^4 = -1982$ and $B_0^6 = +681.7$ (SrF_2); $B_0^4 = -1987$ and $B_0^6 = +487.0$ (PbF_2)). As may be seen in figure 1, these values lead to almost perfect ($\sigma < 1\ cm^{-1}$) reproduction of corresponding experimental energy level splittings.

The data collected in figure 1 also contain one piece of information that turns out to be important further on in our analysis. Examining the energies of the $^7F_3$ levels, we see that the centre of gravity of these levels is shifted by about $100\ cm^{-1}$ upwards in PbF_2, as compared to CdF_2 or SrF_2. Since the level separation is similar in PbF_2, CdF_2 and SrF_2, the two levels seen in PbF_2 are taken to be the same levels (tentatively assumed to be triplets) as those seen in CdF_2 and SrF_2. It thus appears that the position of the barycentre of the $^7F_3$ manifold, and thus the type of dopant–ligand bonding, undergoes a significant change as we move from Eu^{3+} in cubic sites in CdF_2 and SrF_2 to Eu^{3+} in cubic sites in PbF_2.

2.2. Determination of phenomenological values of B_q^k for Dy^{3+}

Optical emission of Dy^{3+} in cubic sites in fluorite-structure hosts has been the subject of a number of investigations in the past [19–22]. Indeed, Al'tshuler *et al* [21] have calculated

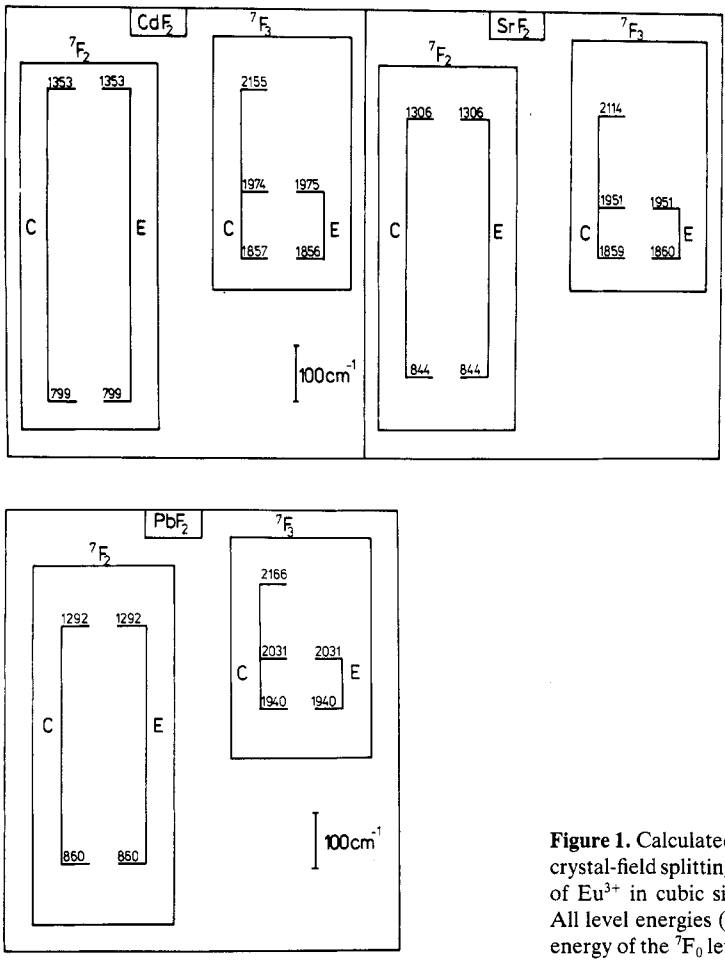

Figure 1. Calculated (C) versus experimental (E) crystal-field splittings of the $^7F_2$ and $^7F_3$ manifolds of Eu^{3+} in cubic sites in CdF_2, SrF_2 and PbF_2. All level energies (cm^{-1}) are with respect to the energy of the $^7F_0$ level.

the relevant crystal-field parameters for Dy^{3+} in a number of these crystals (CdF_2, CaF_2, SrF_2, BaF_2). However, a more sophisticated calculation of the crystal-field parameters of Dy^{3+} in cubic sites in CaF_2 by Nara and Schlesinger [22] led to B_q^k values that were significantly different from those of Al'tshuler *et al* ($B_0^4 = -2192.3$, $B_0^6 = +775.2$ cm^{-1} in [22] as compared with $B_0^4 = -2057$, $B_0^6 = +670$ cm^{-1} in [21]). These differences appear to be large enough to warrant a crystal-field reinvestigation of cubic centres of Dy^{3+} in these hosts.

An examination of the procedure followed by Al'tshuler *et al* [21] shows that in their calculation these authors used perturbation matrices containing all states of the ^6H term of Dy^{3+}. This approach ignores the well known overlap (and consequent strong wavefunction mixing) of some of the higher states of the ^6H term with states of the $^6F_{11/2}$ and $^6F_{9/2}$ manifolds of Dy^{3+} [15, 23]. This point was noted by Nara and Schlesinger [22] as the most likely reason for the difference between the two crystal-field parameter sets. Our investigation showed that it is nevertheless, not necessary to use a fitting procedure as elaborate as theirs to obtain very similar B_q^k values.

We start by recalling that the early calculation of Axe and Dieke [24] showed that *J*-mixing has little apparent effect on the positions of levels of the lowest two (i.e. $^6H_{15/2}$

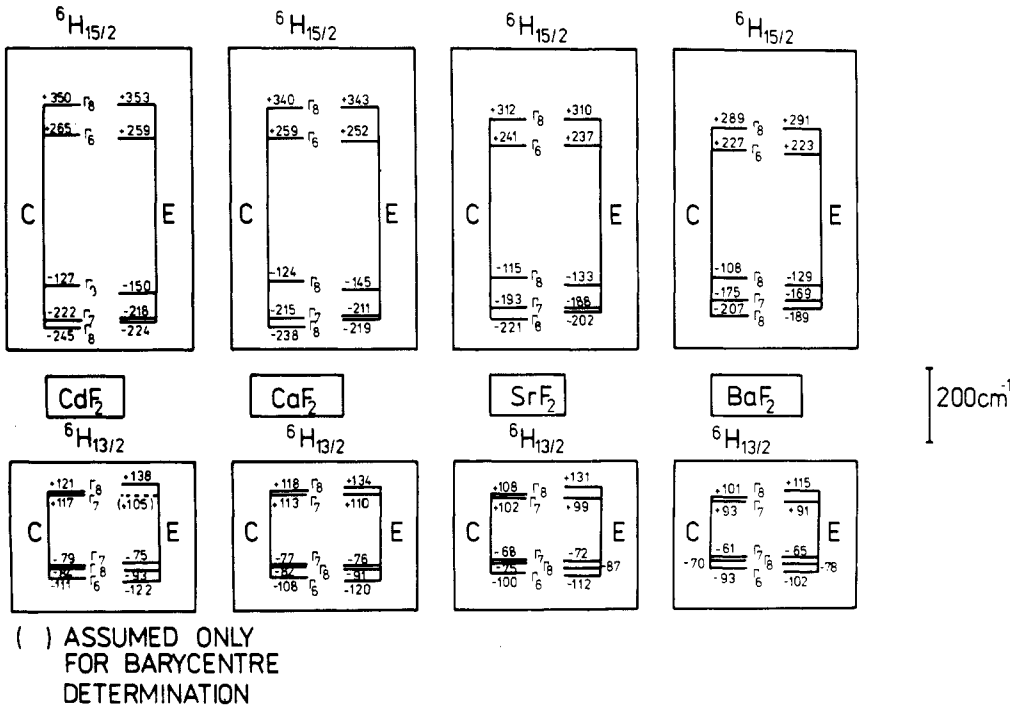

Figure 2. Calculated (C) versus experimental (E) crystal-field splittings of the $^6H_{15/2}$ and $^6H_{13/2}$ manifolds of Dy^{3+} in cubic sites in fluorite-structure hosts. Adjusted RMS deviation σ equals 14.8, 13.2, 14.0 and 12.3 cm^{-1} for cubic sites in, respectively, CdF_2, CaF_2, SrF_2 and BaF_2. All level energies (cm^{-1}) are with respect to the barycentre of the corresponding J-manifold. In order to fix the barycentre of the $^6H_{13/2}$ manifold for CdF_2, the energy of the relevant spectral transition was assumed to be the same as in CaF_2.

and $^6H_{13/2}$) J-manifolds of Dy^{3+}. However, for the next excited manifold ($^6H_{11/2}$), the situation may be expected to be very different. Here, both spin–orbit and crystal-field interactions with states of the relatively close-lying (energy separation of approximately 1700 cm^{-1}) $^6F_{11/2}$ manifold are significant, and should be included in a calculation in which accurate values of B_q^k are sought. We thus expected that a simpler way to obtain phenomenological B_q^k values close to those resulting when all the ^6H and ^6F states are accounted for would be to use a perturbation matrix containing only the $^6H_{15/2}$ and $^6H_{13/2}$ states, with J-mixing ignored.

Bearing in mind the above considerations, we employed the latter procedure in parametrising the energy level scheme established for the $^6H_{15/2}$ and $^6H_{13/2}$ manifolds of Dy^{3+} in a cubic site in CaF_2 by Al'tshuler *et al* [21]. The resulting B_q^k parameter values ($B_0^4 = -2185\ cm^{-1}$, $B_0^6 = +733.6\ cm^{-1}$) did indeed turn out to be close to those obtained by Nara and Schlesinger [22]. As expected, extending the fitting basis by adding states of the $^6H_{11/2}$ manifold made the agreement worse, resulting in phenomenological B_q^k values closer to those of Al'tshuler *et al* ($B_0^4 = -2135\ cm^{-1}$, $B_0^6 = +677.0\ cm^{-1}$). In further calculations we therefore fitted only the centre-of-manifold splittings of the $^6H_{15/2}$ and $^6H_{13/2}$ manifolds (using the data from [21]), performing simultaneous diagonalisation of the two relevant perturbation matrices (of dimensions 16×16 and 14×14).

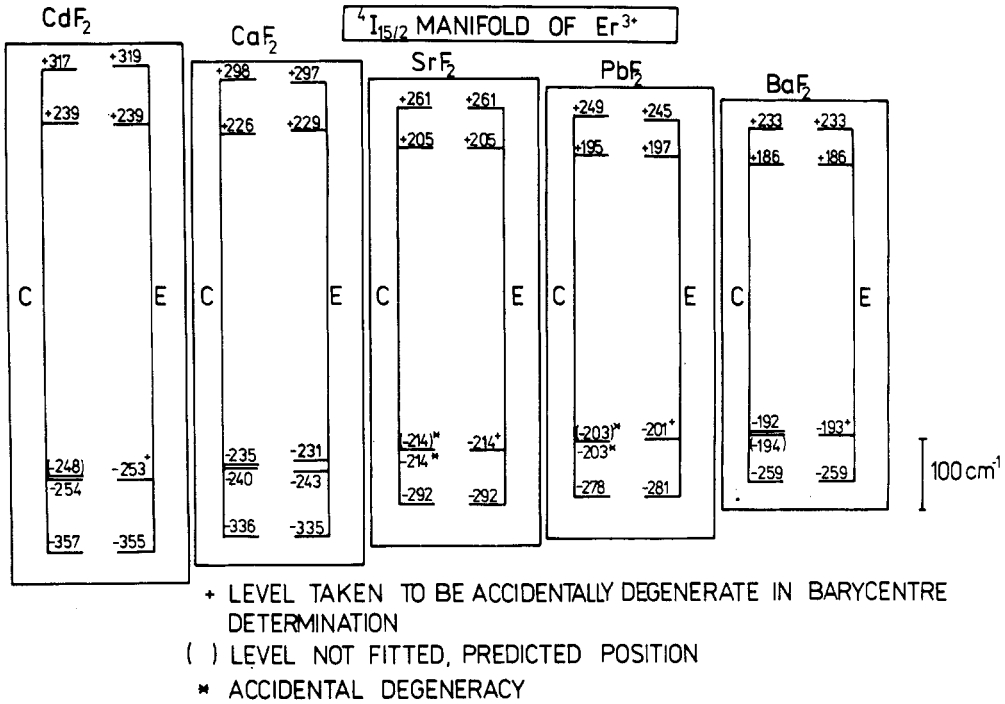

Figure 3. Calculated (C) versus experimental (E) crystal-field splittings of the $^4I_{15/2}$ manifold of Er^{3+} in cubic sites in fluorite-structure hosts. Adjusted RMS deviation σ equals 2.1, 3.3, <1, 4.0 and <1 cm^{-1} for cubic sites in, respectively, CdF_2, CaF_2, SrF_2, PbF_2 and BaF_2. All level energies (cm^{-1}) are with respect to the barycentre of the $^4I_{15/2}$ manifold.

The centre-of-manifold splittings calculated in this way for Dy^{3+} in cubic sites in CdF_2, CaF_2, SrF_2 and BaF_2 are shown in figure 2. The corresponding independent and non-zero B_q^k values are (in cm^{-1}): $B_0^4 = -2245$, $B_0^6 = +757.1$ (CdF_2); $B_0^4 = -2185$, $B_0^6 = +733.6$ (CaF_2); $B_0^4 = -2029$, $B_0^6 = +654.8$ (SrF_2); $B_0^4 = -1905$, $B_0^6 = +590.4$ (BaF_2).

2.3. Determination of phenomenological values of B_q^k for Er^{3+}

An early calculation of the crystal-field parameters of Er^{3+} in cubic sites in CaF_2, SrF_2, PbF_2 and BaF_2 was made by Aizenberg *et al* [25]. This calculation was performed on the basis of the four measured level energies of the ground $^4I_{15/2}$ manifold of Er^{3+} in these systems. However, in the period since that investigation was carried out, new experimental data have accumulated. In particular, Moore [26] observed the fifth level of the $^4I_{15/2}$ manifold of Er^{3+} in cubic sites in CaF_2 (i.e. the last one expected from group-theory arguments), whereas Mho and Wright performed site-selective studies of the Er^{3+}:CdF_2 [27] and Er^{3+}:PbF_2 [28] systems. In view of these developments, a new calculation of crystal-field parameter values for Er^{3+}:fluorite systems was clearly desirable.

In their calculation, Aizenberg *et al* [25] assumed that only four $^4I_{15/2}$ levels were seen, since the Γ_6 level and one of the Γ_8 levels are accidentally degenerate. For the case

of CaF_2, Moore [26] showed that this is only close to the truth (the two levels were found to be separated by 12 cm^{-1}). We therefore chose to test this assumption, and took the observed level to be the Γ_8 level, making the energy of the Γ_6 level a prediction of our calculation. Accidental degeneracy of these two levels was assumed *only for barycentre determination*.

Thus, phenomenological B_q^k values were determined by fitting the centre-of-manifold energies of four (or five in the case of CaF_2) levels of the ground $^4I_{15/2}$ manifold. The results of this calculation may be seen in figure 3. The corresponding B_q^k values are (in cm^{-1}): $B_0^4 = -2007$, $B_0^6 = +691.0$ (CdF_2); $B_0^4 = -1906$, $B_0^6 = +650.5$ (CaF_2); $B_0^4 = -1755$, $B_0^6 = +567.4$ (SrF_2); $B_0^4 = -1664$, $B_0^6 = +540.2$ (PbF_2); $B_0^4 = -1601$, $B_0^6 = +504.6$ (BaF_2). Moreover, our results indicate that the Γ_8 and Γ_6 levels are accidentally degenerate in SrF_2 and PbF_2, and very nearly so in BaF_2. Thus, only in the case of CdF_2 (and, perhaps, BaF_2) does there appear to be a chance of observing an additional $^4I_{15/2}$ manifold level of Er^{3+}.

3. Reconstruction of local lattice distortions

We start our description of the procedure followed in translating phenomenological B_q^k values into information about local host-lattice distortions from an expression (used in [10, 11]) linking the crystal-field parameters with electrostatic lattice sums for the centre of interest:

$$B_q^k = \tau^{-k}\langle r^k\rangle(1 - \sigma_k)A_q^k \tag{1}$$

with $\langle r^k\rangle$ and σ_k being, respectively, the relevant free-ion radial integral (the numerical values used come from the calculation of Freeman and Watson [29]) and the Sternheimer shielding factor (we use values extrapolated linearly from those of Erdös and Kang [30]). The quantity τ is an empirical scaling factor, meant to account both for inaccuracy of free-ion Hartree–Fock $\langle r^k\rangle$ values as well as for the effect of additional wavefunction expansion in a host lattice.

The final quantity in (1) is the electrostatic lattice sum A_q^k. In calculating this, we divide the lattice into two regions—the region in which lattice ions undergo relaxation (region I), and that in which they remain at their ideal lattice sites (region II). For the cubic sites of RE^{3+} ions in fluorite-structure hosts, it appears that relaxation of non-ligand lattice ions may, to a good approximation, be neglected [1, 31], and we therefore limit region I to the eight nearest neighbours of the dopant. Moreover, since local cubic symmetry appears to hold for these centres [1], we take the relaxation in region I to be purely radial, and to be the same for each of the relaxing ligands. Each of these eight relaxing F^- ions is assigned effective charge Q, whose value is to be determined from phenomenological values of B_q^k.

As far as ions in region II are concerned, we take them to be rigid valence charges, and use the results of Vetri and Bassani [32] to calculate their contribution to A_q^k.

We thus obtain the following expression for A_q^k:

$$A_q^k = (QS_q^k/R^{k+1}) + A_{q,\text{rest}}^k \tag{2}$$

where Q is the ligand effective charge, S_q^k is a numerical factor depending on ligand angular coordinates, R is the dopant–ligand separation and $A_{q,\text{rest}}^k$ is the electrostatic lattice sum for the ions in region II.

From the above discussion, we see that values of three quantities (τ, Q and R) are to be obtained from experimental data. However, since we have only two independent non-zero B_q^k values to work with, one of the three empirical quantities sought should be derived without recourse to the B_q^k values for the cubic centre studied.

Fortunately, a closer investigation of the problem [33] shows that values of τ would, in any case, be only weakly, if at all, dependent on which particular fluorite host lattice is being studied. This is due to the fact that by far the largest contribution to τ appears to come from the inaccuracy of free-ion Hartree–Fock $\langle r^k \rangle$ values [34], an effect that is clearly host-lattice-independent. Moreover, the additional contributions to τ arising as a result of ligand charge penetration should be similar for a series of similar hosts, such as the fluorite-structure crystals studied here.

We are thus led to conclude that τ may, to a good approximation, be taken to be host-lattice-independent. It is unclear at this point whether this independence is a good approximation only for hosts from the fluorite-structure family, or remains valid for any host. In further calculations we shall employ values of τ obtained by Leavitt *et al* [35]. These values were obtained by parametrising the spectra of RE^{3+} dopants in $CaWO_4$, and we thus assume at this stage that the host independence of values of τ is valid for *any* host, i.e. *not only* within the fluorite crystal family. We shall return to this matter in section 4.

Elimination of τ from the set of parameters that need to be determined allows us to translate meaningfully, using equations (1) and (2), the B_0^4 and B_0^6 values for a given cubic centre into model values of Q and R. We followed this procedure, with the values of B_q^k used coming from the calculations reported in section 2 in the case of Eu^{3+}, Dy^{3+} and Er^{3+}; from the work of Davydova *et al* [12] for Tb^{3+}; and from that of O'Hare *et al* [13] for Gd^{3+}. The resulting values of Q and R are collected in table 1.

4. Discussion of the results

A comparison of the dopant–ligand separations calculated using the procedure outlined in section 3 (column IV in table 1) and the relevant ideal lattice distances (column I) shows that, according to our results, significant local lattice collapse does appear to take place in the centres of interest. The size of this effect appears to vary from host to host, the magnitude of the relaxation apparently increasing with increasing host lattice constant. As a result, in the majority of cases, the distance from the rare-earth dopant to the ligands remains approximately constant as we move across the CdF_2–CaF_2–SrF_2–PbF_2–BaF_2 host sequence. Thus, most of the variation in the crystal-field parameter values comes from variation in values of the effective charge Q.

The first problem that needs to be addressed in connection with the above results is whether the above model distances are anywhere close to real ones in magnitude. This question arises directly from our discussion of the validity of adopting values of τ established for $CaWO_4$ when dealing with fluorite hosts. In the apparent absence of direct experimental measurements of these separations, we are forced to adopt the second best method of evaluating the correctness of our model predictions, i.e. we compare them with results of other calculations. Thus, in table 1, we show the dopant–ligand separations for the centres of interest, calculated using two different local distortion models. These data show that our model procedure leads to values of the separations close in magnitude to those predicted by the other models considered. We

Table 1. Ligand effective charges and dopant–ligand separations in cubic centres in fluorite-structure hosts.

System		Dopant–ligand separation (Å)[a]				Effective charge
Dopant	Lattice	I	II	III	IV	
Er^{3+}	CdF_2	2.333	2.24	2.297	2.163	0.753
Er^{3+}	CaF_2	2.366	2.26	2.307	2.168	0.722
Er^{3+}	SrF_2	2.511	2.27	2.337	2.184	0.675
Er^{3+}	PbF_2	2.566	2.25	2.337	2.169	0.614
Er^{3+}	BaF_2	2.685	2.22	2.366	2.174	0.589
Dy^{3+}	CdF_2	2.333	2.27	2.316	2.302	0.982
Dy^{3+}	CaF_2	2.366	2.29	2.325	2.296	0.937
Dy^{3+}	SrF_2	2.511	2.30	2.355	2.290	0.840
Dy^{3+}	BaF_2	2.685	2.25	2.386	2.291	0.772
Tb^{3+}	CaF_2	2.366	2.30	2.335	2.222	0.758
Tb^{3+}	SrF_2	2.511	2.31	2.365	2.207	0.683
Tb^{3+}	PbF_2	2.566	2.29	2.365	2.210	0.653
Tb^{3+}	BaF_2	2.685	2.26	2.395	2.190	0.596
Gd^{3+}	CaF_2	2.366	2.32	2.346	2.184	0.726
Gd^{3+}	SrF_2	2.511	2.33	2.377	2.211	0.672
Gd^{3+}	BaF_2	2.685	2.28	2.408	2.278	0.689
Eu^{3+}	CdF_2	2.333	2.31	2.343	2.279	0.888
Eu^{3+}	SrF_2	2.511	2.34	2.384	2.252	0.714
Eu^{3+}	PbF_2	2.566	2.32	2.385	2.669	1.658

[a] The columns under this heading show:
I—distance in an undistorted lattice [1];
II—distance obtained by subtracting from I the difference in the ionic radii of the relevant lattice cation and the RE^{3+} ion [36];
III—results of a shell-model calculation [37];
IV—results of the present work.

take this as an indication that the values of τ used in our work are close to the correct ones.

To test the results of our modelling procedure further, we may compare these with some (albeit limited) deductions from magnetic resonance data. Thus, table 2 contains a comparison of the relative dopant–ligand distances for the cubic centres of Gd^{3+} calculated by Baker [31] (columns I–III) and obtained in this work. We see that the values calculated in the present study are strikingly close to those deduced from magnetic resonance data.

For the cubic centres of Gd^{3+} in the fluorites, we may also compare the picture of local lattice distortions resulting from the present study with results of several independent calculations of ligand displacements in these centres. This possibility appears to be a result of the interest of many researchers in half-filled-shell dopants (see, for example, the review by Newman and Urban [39]). Such a comparison is made in table 3, the ligand displacements resulting from the present modelling procedure being compared with the appropriate values calculated by Tovar *et al* [37] and Yeung [40], and with the values interpolated from the results of Ivanenko and Malkin [41] by Edgar and Newman [42]. This comparison shows that both the present study and the calculations of both Tovar

Table 2. Relative dopant–ligand distances in the cubic centres of Gd^{3+} in the fluorites. Results of the present investigation are compared with relevant values deduced from magnetic resonance data by Baker [31].

	Change in Gd^{3+}–ligand distance relative to CaF_2 (pm)[a]				
Host crystal	Ideal lattice	I	II	III	Present calculation
CaF_2	Zero (by definition)				
SrF_2	+14.5	+2.8	+2.5	+3.0	+2.7
BaF_2	+31.9	+5.5	+5.5	+8.7	+9.4

[a] Columns show:
I—figure 2 of [31];
II—method of Baberschke [38];
III—figure 3 of [31].

Table 3. Calculated ligand displacements from ideal lattice positions in cubic centres of Gd^{3+} in the fluorites.

	Ligand displacement (Å)[a]			
Host crystal	I	II	III	Present calculation
CaF_2	−0.012	−0.029	+0.003	−0.182
SrF_2	−0.126	−0.152	−0.090	−0.300
BaF_2	−0.267	−0.317	−0.282	−0.407

[a] Columns show:
I—shell-model calculation [37];
II—Yeung [40];
III—interpolation from the results of Ivanenko and Malkin [41, 42].

et al and Yeung agree in predicting that, for all three centres considered, the ligands move towards the dopant, and the magnitude of their displacement from ideal lattice positions increases with increasing host lattice constant. The apparent difference in the calculated magnitudes of the ligand displacements may be ascribed to a need to modify slightly the value of τ for Gd^{3+} used in the present calculation (as was to be expected since the values of τ used were the correct ones for $CaWO_4$). On the other hand, the fact that the ligand displacements resulting from the present calculation are that close to results of other studies may be taken as yet another indication of the fact that values of τ are, to a good approximation, lattice-independent. It may, moreover, be noted that the changes in ligand displacement in going from one fluorite host to another are similar in all the calculations compared in table 3.

Examining the ligand displacements calculated for the cubic centre of Gd^{3+} in CaF_2, we see that both the result of present work and those of Tovar *et al* and Yeung are in qualitative disagreement with the ligand displacement interpolated from the results of Ivanenko and Malkin. This result of the present calculation thus appears to reinforce the doubts advanced in the past [42] about the correctness of the Ivanenko and Malkin picture of local lattice distortions in the cubic centres of rare-earth ions in the fluorites.

Finally, the data in table 1 show that there is one instance of marked departure from general trends in R and Q values. For the case of the cubic centre in the Eu^{3+}:PbF_2 system, the model dopant–ligand distance comes out to be larger than it would be in an ideal lattice. Moreover, the value of Q for this system is much larger than unity, in sharp contrast to the corresponding values for the other systems (always less than one). We thus see that the assumptions that underlie our calculation apparently break down when we move to a system in which a significantly different type of dopant–ligand bonding is realised.

The above observation may be viewed in the context of the ongoing debate about the utility of the semi-empirical schemes developed within the electrostatic crystal-field model, from the point of view of analysing the spectra of rare-earth dopants in solid-state hosts. A full account of the current stage of this debate is clearly beyond the scope of this paper (recent expositions of the divergent points of view in this matter may be found in the reviews by Morrison and Leavitt [43] and Newman and Ng [44]), but our results for the cubic centre of Eu^{3+} in PbF_2 appear to underline one consideration that should be kept in mind in this dispute. The basic assumption underlying the electrostatic crystal-field model is that the perturbing potential may be treated as a small external perturbation of the free-ion states of the dopant. The fact that the barycentres of the J-manifolds of a given dopant remain practically unchanged in going from one host to another is usually taken as an indication of the essentially free-ion nature of the states of the 4f configuration. Thus, situations when sizable barycentre shifts appear in going from one host to another pose serious problems for the electrostatic model and, as we saw for the case of the cubic centres of Eu^{3+} in the fluorites, may lead to breakdown of lattice simulation schemes formulated within the electrostatic framework.

5. Conclusions

Results of the present study reinforce our former conclusion [10] that a realistic picture of local lattice relaxation in the centres formed when rare-earth dopants are introduced into fluorite hosts may be deduced from relevant phenomenological crystal-field parameter values. For more complex (and thus lower-symmetry) centres, the need to reconstruct more complex lattice relaxation patterns is then compensated by availability of more numerous independent phenomenological crystal-field parameter values, and the problem thus remains tractable.

We should note, in this context, that results of present calculations suggest caution when extending the procedures developed for some of these systems to those of the others that are characterised by significantly different dopant–ligand bonding.

Acknowledgments

The author wishes to thank G D Jones for supplying some unpublished data relevant to the present investigation, M Godlewski for some stimulating discussions and J M Langer for a critical reading of the manuscript of this paper. This work was supported by funds from programme CPBP 01.12.

References

[1] Hayes W (ed) 1974 *Crystals with the Fluorite Structure* (Oxford: Clarendon) chs 5 and 6
[2] Weber M J and Bierig R W 1964 *Phys. Rev.* **134** A1492
[3] Zakharchenya B P and Rusanov I B 1966 *Sov. Phys.–Solid State* **8** 31
[4] Rector C W, Pandey B C and Moos H W 1966 *J. Chem. Phys.* **45** 171
[5] Baker J M and Wood R L 1980 *J. Phys. C: Solid State Phys.* **13** 4751
[6] Moore D S and Wright J C 1981 *J. Chem. Phys.* **74** 1626
[7] Hamers R J, Wietfeldt J R and Wright J C 1982 *J. Chem. Phys.* **77** 683
[8] Mho S I and Wright J C 1982 *J. Chem. Phys.* **77** 1183
[9] Weesner F J, Wright J C and Fontanella J J 1986 *Phys. Rev.* B **33** 1372
[10] Leśniak K 1986 *J. Phys. C: Solid State Phys.* **19** 2721
[11] Leśniak K 1988 *J. Opt. Soc. Am.* B **5** 1266
[12] Davydova M P, Stolov A L and Shcherbakov V D 1976 *Sov. Phys.–Solid State* **18** 1656
[13] O'Hare J M, Detrio J A and Donlan V L 1969 *J. Chem. Phys.* **51** 3937
[14] Wybourne B G 1965 *Spectroscopic Properties of Rare Earths* (New York: Wiley Interscience)
[15] Carnall W T, Crosswhite H and Crosswhite H M 1977 Energy level structure and transition probabilities of the trivalent lanthanides in LaF_3 *Argonne National Laboratory Report*
[16] Jouart J P, Bissieux C and Mary G 1987 *J. Lumin.* **37** 159
[17] Jouart J P, Bissieux C, Egee M, Mary G and de Murcia M 1981 *J. Phys. C: Solid State Phys.* **14** 4923
[18] Jouart J P, Bissieux C, Mary G and Egee M 1985 *J. Phys. C: Solid State Phys.* **18** 1539
[19] Kiss Z J and Staebler D L 1965 *Phys. Rev. Lett.* **14** 691
[20] Merz J L and Pershan P S 1967 *Phys. Rev.* **162** 217
[21] Al'tshuler N S, Eremin M V, Luks R K and Stolov A L 1970 *Sov. Phys.–Solid State* **11** 2921
[22] Nara H and Schlesinger M 1971 *Solid State Commun.* **9** 1247
[23] Wybourne B G 1962 *J. Chem. Phys.* **36** 2301
[24] Axe J D and Dieke G H 1962 *J. Chem. Phys.* **37** 2364
[25] Aizenberg I B, Malkin B Z and Stolov A L 1972 *Sov. Phys.–Solid State* **13** 2155
[26] Moore D S 1980 *PhD Thesis* University of Wisconsin (unpublished)
[27] Mho S I and Wright J C 1984 *J. Chem. Phys.* **81** 1421
[28] Mho S I and Wright J C 1983 *J. Chem. Phys.* **79** 3962
[29] Freeman A J and Watson R E 1962 *Phys. Rev.* **127** 2058
[30] Erdös P and Kang J H 1972 *Phys. Rev.* B **6** 3393
[31] Baker J M 1979 *J. Phys. C: Solid State Phys.* **12** 4039
[32] Vetri G and Bassani F 1968 *Nuovo Cim.* **55B** 504
[33] Leśniak K 1989 *Acta Phys. Polon.* A **75** 169
[34] Karayianis N and Morrison C A 1975 *Harry Diamond Laboratories Report* no. TR-1682
[35] Leavitt R P, Morrison C A and Wortman D E 1975 *Harry Diamond Laboratories Report* no. TR-1673
[36] Tennent R M (ed) 1974 *Science Data Book* (Edinburgh: Oliver and Boyd)
[37] Tovar M, Ramos C A and Fainstein C 1983 *Phys. Rev.* B **28** 4813
[38] Baberschke K 1971 *Z. Phys.* **252** 65
[39] Newman D J and Urban W 1975 *Adv. Phys.* **24** 793
[40] Yeung Y Y 1988 *J. Phys. C: Solid State Phys.* **21** L549
[41] Ivanenko Z I and Malkin B Z 1969 *Sov. Phys.–Solid State* **11** 1498
[42] Edgar A and Newman D J 1975 *J. Phys. C: Solid State Phys.* **8** 4023
[43] Morrison C A and Leavitt R P 1982 *Handbook on the Physics and Chemistry of Rare-Earths* vol 5, ed K A Gschneidner and L Eyring (Amsterdam: North-Holland) p 461
[44] Newman D J and Ng B 1989 *Rep. Prog. Phys.* **52** 699